Charmless hadronic B decays into Vector, Axial Vector and Tensor final states at BaBar

Paolo Gandini (On behalf of the *BABAR* Collaboration)
Università degli Studi and INFN Milano, via Celoria 16, I-20133 Milano, Italy

We present experimental measurements of branching fraction and longitudinal polarization fraction in charmless hadronic B decays into vector, axial vector and tensor final states with the final dataset of *BABAR*. Measurements of such kind of decays are a powerful tool both to test the Standard Model and search possible sources of new physics.

1. Introduction

In this document we present a short review of the last experimental results at *BABAR* concerning charmless quasi two-body decays in final states containing particles with *spin 1* or *spin 2* and different parities. This kind of decays has received considerable theoretical interest in the last few years [1, 2, 3] and this particular attention has led to interesting experimental results at the current *b-factories*. In fact, the study of longitudinal polarization fraction f_L in charmless B decays to vector vector (VV), vector axial-vector (VA) and axial-vector axial-vector (AA) mesons provides information on the underlying helicity structure of the decay mechanism. Naïve helicity conservation arguments predict a dominant longitudinal polarization fraction $f_L \sim 1$ for both tree and penguin dominated decays and this pattern seems to be confirmed by tree-dominated $B \to \rho\rho$ [4] and $B^+ \to \omega\rho^+$ [5] decays. Other penguin dominated decays, instead, show a different behavior: the measured value of $f_L \sim 0.5$ in $B \to \phi K^*$ decays [6] is in contrast with naïve Standard Model (SM) calculations. Several solutions have been proposed such as the introduction of non-factorizable terms and penguin-annihilation amplitudes [7], while other explanations invoke new physics [8]. New modes have been investigated to shed more light on the problem.

2. Helicity Amplitudes

The polarization fraction is extracted from data introducing some angular information describing the decay process. The easiest way to study angular distributions is in terms of helicity amplitudes: total angular momentum must be conserved in $(Spin-0) \to (Spin-1)+(Spin-1)$ decays (similar arguments can be used for $(Spin-0) \to (Spin-1)+(Spin-2)$ decays), so orbital L must be 0, 1 or 2 while $\vec{J}_{tot}$ projection along the flight direction of the daughter mesons must be equal to 0. This suggests that the helicities of both daughter mesons must be the same (1, 0 or -1); so the decay process can be described by three different amplitudes Λ_1 Λ_0 and Λ_{-1}. The polarization of the two intermediate mesons can be commonly measured introducing angular distributions as shown in Fig. 1. For 2-body decays we define the angle θ_i as the angle between the direction of the recoiling B and the direction of one of the resonance daughters, while for 3-body decays we use the angle between the normal to the decay plane with respect tho the other resonance daughter. Due to the limited number of expected signal events in charmless hadronic decays we do not perform a full angular analysis of the decay and we integrate on the angle ϕ between the two planes of the decaying particles, leading to a non-trivial dependence on a single parameter

$$f_L = \frac{|\Lambda_0|^2}{\sum_{i=-1}^{1}|\Lambda_i|^2}$$

We find these angular distributions for our decays:

$$\frac{\mathrm{d}\Gamma}{\mathrm{d}\cos\theta_1 \mathrm{d}\cos\theta 2} \propto$$

$$\begin{cases} B \to VV & f_L \cos^2\theta_1 \cos^2\theta_2 + \frac{1}{4} f_T \sin^2\theta_1 \sin^2\theta_2 \\ B \to AA & f_L \sin^2\theta_1 \sin^2\theta_2 + \frac{1}{4}(1+\cos^2\theta_1)(1+\cos^2\theta_2) \\ B \to VT & f_L \frac{1}{3}\cos^2\theta_1 (3\cos^2\theta_2 - 1)^2 + f_T \sin^2\theta_1 \sin^2\theta_2 \cos^2\theta_2 \\ \ldots \end{cases}$$

where f_L and $f_T = 1 - f_L$ can be fitted from data.

3. Analysis Techniques

The results presented here are based on data collected with the *BABAR* detector [9] at the PEP-II asymmetric-energy e^+e^- collider [10], located at the SLAC National Accelerator Laboratory. $B\overline{B}$ pairs are recorded at the $\Upsilon(4S)$ resonance at a center-of-mass energy of $\sqrt{s} = 10.58$ GeV.

Background in our analyses arises primarily from random track combinations in continuum events ($e^+e^- \to q\overline{q}$, with $q = u, d, s, c$), where a pair of light quarks is produced. We reduce this background by using optimized cuts on event shape variables, such as the angle θ_T between the thrust axis of the B candidate and the thrust axis of the rest of the event: the distribution of $|\cos\theta_{\mathrm{T}}|$ is sharply peaked near 1 for

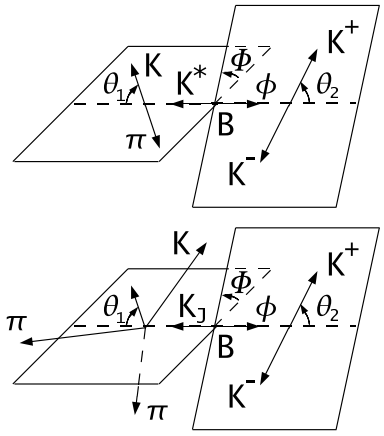

Figure 1: Definition of the decay angles θ_1 and θ_2 given in the rest frames of the decaying parents for 2-body and 3-body decays.

combinations drawn from jet-like continuum events and is nearly uniform for $B\overline{B}$ events. Additional cuts are applied on the invariant masses of the decaying particles, the χ^2 probability of the B vertex fit, while we impose particle identification requirements to ensure a good $K/\pi/p$ separation. A B meson candidate is kinematically characterized by the energy-substituted mass $m_{\rm ES} \equiv \sqrt{(s/2 + \mathbf{p}_0 \cdot \mathbf{p}_B)^2/E_0^2 - \mathbf{p}_B^2}$ and energy difference $\Delta E \equiv E_B^* - \sqrt{s}/2$, where the subscripts 0 and B refer to the initial $\Upsilon(4S)$ and the B candidate in the laboratory frame, respectively, and the asterisk denotes the $\Upsilon(4S)$ frame. $m_{\rm ES}$ and ΔE distributions are sharply peaked for signal, while they are almost flat for $q\overline{q}$ background. Background can also arise from $B\overline{B}$ events, which are taken into account with detailed Monte Carlo simulations.

Results are obtained extracting the number of signal events from an unbinned extended maximum-likelihood (ML) fit with input variables $m_{\rm ES}$, ΔE, the invariant masses of the decaying particles, the helicity angles defined above and the output of a Fisher discriminant (or a neural network) obtained combining different event shape variables.
The likelihood function is:

$$\mathcal{L} = e^{-\left(\sum_{j=1}^{hyp} n_j\right)} \prod_{i=1}^{N} \left[\sum_{j=1}^{hyp} n_j \mathcal{P}_j(\mathbf{x}_i) \right], \qquad (1)$$

where N is the number of input events, n_j is the number of events for the hypothesis j (signal or background) and $\mathcal{P}_j(\mathbf{x}_i)$ is the corresponding probability density function (PDF), evaluated with the observables $\mathbf{x}_i$ of the ith event.

4. Experimental Results

4.1. $B^0 \to a_1(1260)^+ a_1(1260)^-$

We present the first measurements of the branching fraction and polarization in $B^0 \to a_1^+ a_1^-$ decays[1], with $a_1^\pm$ decaying into three charged pions [11]. For this mode, the only available experimental information is a branching fraction upper limit (UL) of 2.8×10^{-3} at 90% confidence level (CL) measured by CLEO [12], while there are no experimental measurements of f_L in $B \to AA$ decays. Theoretical expectations for the branching fraction range from 37.4×10^{-6} [2] to 6.4×10^{-6} [3], depending on the different approach used, while f_L is predicted to be about 0.64 [2]. In this decay mode we reconstruct $B^0 \to a_1^+ a_1^-$, with $a_1^\pm \to \rho(770)\pi^\pm$ and $\rho(770) \to \pi^+\pi^-$. We do not separate the P-wave $(\pi\pi)_\rho$ and the S-wave $(\pi\pi)_\sigma$ components in the $a_1 \to 3\pi$ decay; a systematic uncertainty is estimated due to the difference in the selection efficiencies. The fit results, presented in Tab. I, are based on an integrated luminosity corresponding to 423 fb^{-1} (equivalent to $(465 \pm 5) \times 10^6$ $B\overline{B}$ pairs).

Signal yield	545 ± 118
Signal yield bias	$+14$
f_L bias	-0.06
S (σ)	5.0
$\mathcal{B}$ ($\times 10^{-6}$)	$47.3 \pm 10.5 \pm 6.3$
f_L	$0.31 \pm 0.22 \pm 0.10$

Table I Fitted signal yield and yield bias (in events), bias on f_L, significance S (including systematic uncertainties), measured branching fraction $\mathcal{B}$ and fraction of longitudinal polarization f_L with statistical and systematic uncertainties.

The significance is the square root of the difference between the value of $-2\ln\mathcal{L}$ (with systematic uncertainties included) for zero signal and the value at its minimum. In this calculation we have taken into account the fact that the floating f_L parameter is not defined in the zero signal hypothesis. The measured branching fraction and longitudinal polarization are in general agreement with QCD factorization expectations [2].

4.2. $B \to b_1 V$ with $V = \rho, K^*$

We search for all charge combinations of decays of a B meson to a final state containing a b_1 meson and a ρ or $K^*(892)$ meson; both neutral and charged B

[1] a_1 notation will be used to indicate the $a_1(1260)$ meson.

decays have been considered [13]. No previous experimental searches for these decays have been reported before. Such B meson decays to charmless AV final states are interesting to be studied experimentally since they may be sensitive to penguin annihilation effects, which tend to enhance certain modes while suppressing others. Branching fractions for AV modes are substantial in several cases, as large as 33×10^{-6} for the $B^0 \to b_1^- \rho^+$ final state [2], so they should be accessible at *BABAR*. Measurements described here are based on an integrated luminosity of 424 fb^{-1}, equivalent to $(465 \pm 5) \times 10^6$ $B\overline{B}$ pairs.

We reconstruct B-meson daughter candidates through the decays $b_1 \to \omega\pi$ (we assume this branching fraction to be 100%), $\omega \to \pi^+\pi^-\pi^0$, $\rho^+ \to \pi^+\pi^0$, $\rho^0 \to \pi^+\pi^-$, $K^{*0} \to K^+\pi^-$, and $K^{*+} \to K^+\pi^0$ or $K^0_S\pi^+$. Results are summarized in Tab. II. We do not observe any statistically significant signal for any of the eight decay modes.

Mode	Y	Y_0	S (σ)	$\mathcal{B}$ & U.L (10^{-6})
$b_1^-\rho^+$	-33 ± 10	4 ± 2	–	$-1.8 \pm 0.5 \pm 1.0$ (<1.4)
$b_1^0\rho^+$	-18 ± 5	-4 ± 2	–	$-3.0 \pm 0.9 \pm 1.8$ (<3.3)
$b_1^+\rho^0$	37 ± 25	8 ± 4	0.4	$1.5 \pm 1.5 \pm 2.2$ (<5.2)
$b_1^0\rho^0$	-8 ± 19	5 ± 3	–	$-1.1 \pm 1.7^{+1.4}_{-0.9}$ (<3.4)
$b_1^- K^{*+}$			1.7	$2.4^{+1.5}_{-1.3} \pm 1.0$ (<5.0)
$b_1^- K^{*+}_{K^+\pi^0}$	3 ± 8	-5 ± 3	0.9	$1.8 \pm 1.9 \pm 1.4$
$b_1^- K^{*+}_{K^0_S\pi^+}$	17 ± 9	4 ± 2	1.5	$3.2 \pm 2.1^{+1.0}_{-1.5}$
$b_1^0 K^{*+}$			0.1	$0.4^{+2.0+3.0}_{-1.5-2.6}$ (<6.7)
$b_1^0 K^{*+}_{K^+\pi^0}$	-8 ± 7	-3 ± 2	–	$-2.2 \pm 3.0^{+5.0}_{-2.3}$
$b_1^0 K^{*+}_{K^0_S\pi^+}$	3 ± 4	0 ± 0	0.4	$1.6 \pm 2.5 \pm 3.3$
$b_1^+ K^{*0}$	55 ± 21	15 ± 8	1.5	$2.9 \pm 1.5 \pm 1.5$ (<5.9)
$b_1^0 K^{*0}$	30 ± 15	-6 ± 3	2.0	$4.8 \pm 1.9^{+1.5}_{-2.2}$ (<8.0)

Table II Signal yield Y (events) and its statistical uncertainty, bias Y_0 (evts), significance S (including systematic uncertainties) and central value of the branching fraction $\mathcal{B}$ with associated upper limit (U.L.) at 90% C.L.

These results are in good agreement with the small predictions from naïve factorization calculations [3], but they are much smaller than the predictions from the more complete QCD factorization calculations [2].

4.3. $B \to \omega V$ with $V = K^*, \rho, f_0$

We report measurements of B decays to the final states ωK^*, $\omega\rho$, and $\omega f_0(980)$, where K^* includes the spin 0, 1, and 2 states, $K_0^*(1430)$, $K^*(892)$, and $K_2^*(1430)$, respectively [14]. The analyzed data sample corresponds to 465×10^6 $B\overline{B}$ pairs. We measure the branching fractions for nine of these decays, five are observed for the first time; where relevant signal is found we also extract the direct *CP*-violating, time-integrated charge asymmetry and f_L. B-daughter candidates are reconstructed through their decays $\rho^0 \to \pi^+\pi^-$, $f_0(980) \to \pi^+\pi^-$, $\rho^+ \to \pi^+\pi^0$, $K^{*0} \to K^+\pi^-$, $K^{*+} \to K^+\pi^0(K^{*+}_{K^+\pi^0})$, $K^{*+} \to K^0_S\pi^+(K^{*+}_{K^0_S\pi^+})$, $\omega \to \pi^+\pi^-\pi^0$, $\pi^0 \to \gamma\gamma$, and $K_s \to \pi^+\pi^-$. In Tab. III we show for each decay mode the measured $\mathcal{B}$, f_L, and $\mathcal{A}_{ch}$ together with the quantities entering into these computations. For decays with K^{*+} we combine the results from the two K^* decay channels, by adding their values of $-2\ln\mathcal{L}$.

	$\mathcal{B}$ (10^{-6})	$\mathcal{B}$ & UL (10^{-6})	S (σ)
$\omega K^*(892)^0$	$2.2 \pm 0.6 \pm 0.2$	–	4.1
$\omega K^*(892)^+$	$2.4 \pm 1.0 \pm 0.2$	3.8	2.5
$\omega(K\pi)_0^{*0}$	$18.4 \pm 1.8 \pm 1.7$	–	9.8
$\omega(K\pi)_0^{*+}$	$27.5 \pm 3.0 \pm 2.6$	–	9.2
$\omega K_2(1430)^{*0}$	$10.1 \pm 2.0 \pm 1.1$	–	5.0
$\omega K_2(1430)^{*+}$	$21.5 \pm 3.6 \pm 2.4$	–	6.1
ωf_0	$1.0 \pm 0.3 \pm 0.1$	1.5	4.5
$\omega\rho^0$	$0.8 \pm 0.5 \pm 0.2$	1.6	
$\omega\rho^+$	$15.9 \pm 1.6 \pm 1.4$	–	9.8
	A_{ch}	f_L	
$\omega K^*(892)^0$	$+0.45 \pm 0.25 \pm 0.02$	$0.72 \pm 0.14 \pm 0.02$	
$\omega K^*(892)^+$	$+0.29 \pm 0.35 \pm 0.02$	$0.41 \pm 0.18 \pm 0.05$	
$\omega(K\pi)_0^{*0}$	$-0.07 \pm 0.09 \pm 0.02$	–	
$\omega(K\pi)_0^{*+}$	$-0.10 \pm 0.09 \pm 0.02$	–	
$\omega K_2(1430)^{*0}$	$-0.37 \pm 0.17 \pm 0.02$	$0.45 \pm 0.12 \pm 0.02$	
$\omega K_2(1430)^{*+}$	$+0.14 \pm 0.15 \pm 0.02$	$0.56 \pm 0.10 \pm 0.04$	
ωf_0	–	–	
$\omega\rho^0$	–	0.8 fixed	
$\omega\rho^+$	$-0.20 \pm 0.09 \pm 0.02$	$0.90 \pm 0.05 \pm 0.03$	

Table III Results for the modes presented in this section. Up: central value of the branching fraction $\mathcal{B}$ with associated upper limit (U.L.) at 90% C.L. where available and significance S. Down: charge asymmetry A_{ch} and polarization fraction f_L.

4.4. $B^+ \to \overline{K}^{*0}K^{*+}$

We present measurements of the branching fraction and longitudinal polarization for the decay $B^+ \to \overline{K}^{*0}K^{*+}$, with a sample of 467 ± 5 million $B\overline{B}$ pairs collected [15]. The decay $B^+ \to \overline{K}^{*0}K^{*+}$ occurs through both electroweak and gluonic $b \to d$ penguin loops and its branching fraction is expected to be of the same order as $B^0 \to K^{*0}\overline{K}^{*0}$: theorethical predictions based on QCD factorization range from $(0.5^{+0.2+0.4}_{-0.1-0.3}) \times 10^{-6}$ [16] to $(0.6 \pm 0.1 \pm 0.3) \times 10^{-6}$ [2]. The $B^0 \to K^{*0}\overline{K}^{*0}$ branching fraction has been measured to be $(1.28^{+0.35}_{-0.30} \pm 0.11) \times 10^{-6}$ [17], while an upper limit at the 90% confidence level (C.L.) of 2.0×10^{-6} has been recently placed on the $B^0 \to K^{*-}K^{*+}$ branching fraction [18]. The previous experimental upper limit on the $B^+ \to \overline{K}^{*0}K^{*+}$ branching

fraction at the 90% C.L. is $71(48) \times 10^{-6}$ [19], assuming a fully longitudinally (transversely) polarized system. The $B^+ \to \overline{K}^{*0}K^{*+}$ candidates are reconstructed through the decays of $\overline{K}^{*0} \to K^-\pi^+$ and $K^{*+} \to K^0_S\pi^+$ or $K^{*+} \to K^+\pi^0$, with $K^0_S \to \pi^+\pi^-$ and $\pi^0 \to \gamma\gamma$. The results of the ML fits are summarized in Tab. IV.

Final State	$K^-\ \pi^+\ K^0_S\ \pi^+$	$K^-\ \pi^+\ K^+\ \pi^0$
Yields (events):		
Signal	$6.9^{+4.5}_{-3.5}$	$13.9^{+7.6}_{-6.4}$
ML Fit Biases	-0.12	0.08
Efficiencies and $\mathcal{B}$:		
$\epsilon(\%)$	11.44 ± 0.08	7.40 ± 0.08
$\prod \mathcal{B}_i(\%)$	15.37	22.22
f_L	$0.72^{+0.23}_{-0.36} \pm 0.03$	$0.79^{+0.22}_{-0.36} \pm 0.03$
$\mathcal{B}$ $(\times 10^{-6})$	$0.85^{+0.61}_{-0.44} \pm 0.11$	$1.80^{+1.01}_{-0.85} \pm 0.16$
$\mathcal{B}$ Significance S (σ)	2.28	2.18
Combined Results:		
f_L	$0.75^{+0.16}_{-0.26} \pm 0.03$	
$\mathcal{B}$ $(\times 10^{-6})$	$1.2 \pm 0.5 \pm 0.1$	
$\mathcal{B}$ Significance S (σ)	3.7	
$\mathcal{B}_{\rm UL}$ $(\times 10^{-6})$	2.0	

Table IV Results of the fit: signal yield and ML Fit biases, efficiencies and $\mathcal{B}$ for single and combined results.

We compute the branching fractions $\mathcal{B}$ by dividing the bias-corrected yield by the number of $B\overline{B}$ pairs, the reconstruction efficiency ϵ given the fitted f_L, and the secondary branching fractions, which we take to be 2/3 for $\mathcal{B}(\overline{K}^{*0} \to K^-\pi^+)$ and $\mathcal{B}(K^{*+} \to K^0\pi^+)$, 1/3 for $\mathcal{B}(K^{*+} \to K^+\pi^0)$, and $0.5 \times (69.20 \pm 0.05)\%$ for $\mathcal{B}(K^0 \to K^0_S \to \pi^+\pi^-)$. We see a significant excess of events, but no 5σ observation is found; all these measurements are compatible with theoretical predictions.

Acknowledgments

I would like to thank Prof. Fernando Palombo and Dott. Vincenzo Lombardo for their support.

References

[1] K.-C. Yang, Nucl. Phys. B Proc. Suppl. **186**, 399(2009).
[2] H.-Y. Cheng and K.-C. Yang, Phys. Rev. D **78**, 094001 (2008).
[3] G. Calderon *et al.*, Phys. Rev. D **76**, 094019 (2007).
[4] Belle Collaboration, A. Somov *et al.*, Phys. Rev. Lett. **96**, 171801 (2006); *BABAR* Collaboration, B. Aubert *et al.*, Phys. Rev. D **76**, 052007 (2007); Belle Collaboration, J. Zhang *et al.*, Phys. Rev. Lett. **91**, 221801 (2003); *BABAR* Collaboration, B. Aubert *et al.*, arXiv:0901.3522[hep-ex], submitted to Phys. Rev. Lett.
[5] *BABAR* Collaboration, B. Aubert *et al.*, Phys. Rev. D **79**, 052005 (2009).
[6] *BABAR* Collaboration, B. Aubert *et al.*, Phys. Rev. D **78**, 092008 (2008); Belle Collaboration, K. F. Chen *et al.*, Phys. Rev. Lett. **91**, 201801 (2003).
[7] A. L. Kagan, Phys. Lett. B **601**, 151 (2004); C. W. Bauer *et al.*, Phys. Rev. D **70**, 054015 (2004); P. Colangelo, F. De Fazio, and T. N. Pham, Phys. Lett. B **597**, 291 (2004); M. Ladisa *et al.*, Phys. Rev. D **70**, 114025 (2004); H. Y. Cheng, C. K. Chua, and A. Soni, Phys. Rev. D **71**, 014030 (2005); H. N. Li and S. Mishima, Phys. Rev. D **71**, 054025 (2005); C. H. Chen *et al.*, Phys. Rev. D **72**, 054011 (2005); M. Beneke *et al.*, Nucl. Phys. B **774**, 64 (2007).
[8] A. K. Giri and R. Mohanta, Phys. Rev. D **69**, 014008 (2004); E. Alvarez *et al.*, Phys. Rev. D **70**, 115014 (2004); P. K. Das and K. C. Yang, Phys. Rev. D **71**, 094002 (2005); C. H. Chen and C. Q. Geng, Phys. Rev. D **71**, 115004 (2005); Y. D. Yang, R. M. Wang, and G. R. Lu, Phys. Rev. D **72**, 015009 (2005); C. S. Hunger *et al.*, Phys. Rev. D **73**, 034026 (2006); C. H. Chen and C. Q. Geng, Phys. Rev. D **75**, 054010 (2007).
[9] *BABAR* Collaboration, B. Aubert *et al.*, Nucl. Instrum. Methods Phys. Res., Sect. A **479**, 1 (2002).
[10] PEP-II Conceptual Design Report, SLAC-R-418 (1993).
[11] *BABAR* Collaboration, B. Aubert *et al.*, arXiv:0907.1776, submitted to Phys. Rev. Lett.
[12] CLEO Collaboration, D. Bortoletto *et al.*, Phys. Rev. Lett. **62**, 2436 (1989).
[13] *BABAR* Collaboration, B. Aubert *et al.*, arXiv:0907.3485, submitted to Phys. Rev. D -RC
[14] *BABAR* Collaboration, B. Aubert *et al.*, Phys. Rev. D **78**, 052005 (2009);
[15] *BABAR* Collaboration, B. Aubert *et al.*, arXiv:0901.1223, submitted to Phys. Rev. D .
[16] M. Beneke, J. Rohrer and D. Yang, Nucl. Phys. B **774**, 64 (2007).
[17] B. Aubert *et al.* (*BABAR* Collaboration), Phys. Rev. Lett. **100**, 081801 (2008).
[18] B. Aubert *et al.* (*BABAR* Collaboration), Phys. Rev. D **78**, 051103 (2008).
[19] R. Godang *et al.* (CLEO Collaboration), Phys. Rev. Lett. **88**, 021802 (2001).